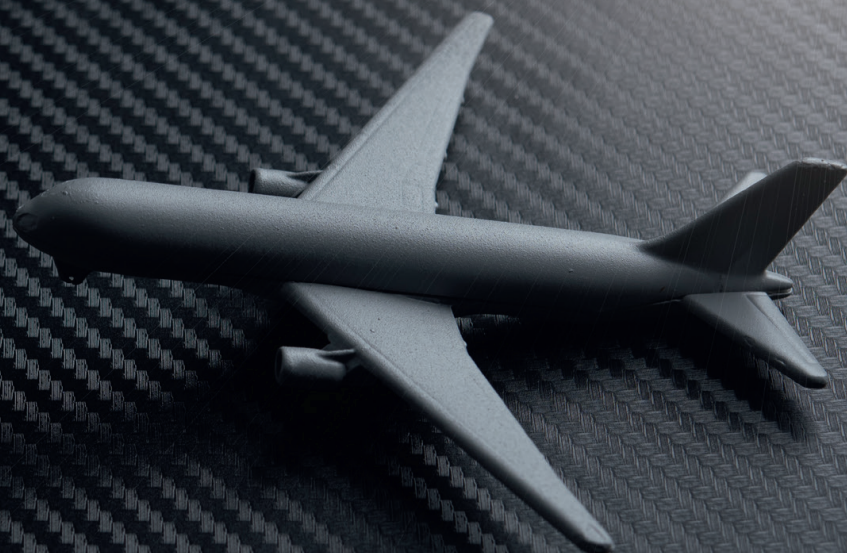**Pēteris Pavlovskis**

ANALYSIS OF TWO ACTUAL PROBLEMS OF INTERLAMINAR FRACTURE ASSESSMENT OF LAYERED COMPOSITE

Summary of the Doctoral Thesis

RIGA TECHNICAL UNIVERSITY

Faculty of Mechanical Engineering, Transport and Aeronautics
Institute of Aeronautics

Pēteris Pavlovskis

Doctoral Student of the Study Programme
"Transport"

ANALYSIS OF TWO ACTUAL PROBLEMS OF INTERLAMINAR FRACTURE ASSESSMENT OF LAYERED COMPOSITE

Summary of the Doctoral Thesis

Scientific supervisor
Dr. habil. sc. ing.
VITĀLIJS PAVELKO

RTU Press
Riga 2022

DOCTORAL THESIS PROPOSED TO RIGA TECHNICAL UNIVERSITY FOR THE PROMOTION TO THE SCIENTIFIC DEGREE OF DOCTOR OF SCIENCE

To be granted the scientific degree of Doctor of Science (Ph. D.), the present Doctoral Thesis has been submitted for the defense at the open meeting of RTU Promotion Council on September 16, 2022 at 14.00 p. m. at the Faculty of Mechanical Engineering, Transport and Aeronautics of Riga Technical University, 6 B Ķīpsalas Str., Room 204.

OFFICIAL REVIEWERS

Lead Researcher Dr. sc. ing. Ali Arshad
Riga Technical University

Professor Dr. habil. sc. ing. Krzysztof Szafran
Institute of Aviation, Poland

Professor Dr. sc. ing. Rafal Chatys
Technical University of Kielce, Poland

DECLARATION OF ACADEMIC INTEGRITY

I hereby declare that the Doctoral Thesis submitted for the review to Riga Technical University for the promotion to the scientific degree of Doctor of Science (Ph. D.) is my own. I confirm that this Doctoral Thesis had not been submitted to any other university for the promotion to a scientific degree.

Pēteris Pavlovskis ……………………………. (signature)
Date: ………………………

The Doctoral Thesis has been written in English. It consists of an Introduction, 5 chapters, Conclusions, 61 figures,3 tables; the total number of pages is 99. The Bibliography contains 108 titles.

CONTENTS

LIST OF ABBREVIATIONS

ASTM – American Society for Testing and Materials
CCM – compliance calibration
CFRP – carbon fiber reinforced polymer
DCB – double-cantilever beam
ESIS – European Structural Integrity Society
GFRP – glass fiber reinforced polymer
MBT – modified beam theory

1. GENERAL CHARACTERISTICS OF THE THESIS

1.1. Relevance of Thesis

Layered composites are widely used in modern aircraft structure. Effective methods of finite element analysis of the stress-strain state of complex parts of the bearing structure have been created, which allows to predict their strength and rigidity with high accuracy. Methods and standards have been developed for determining the mechanical characteristics of materials which are a key component of the calculation complex for assessing the bearing capacity of a modern aircraft.

Naturally, the computational and design complex of the aircraft structure is in continuous development and improvement as the scientific problems put forward by practice are solved.

In particular, to determine the interlaminar fracture toughness of a layered composite, there is an American Society for Testing and Materials standard based on the use of a linear model of bending of a double-cantilever beam specimen. The standard contains several restrictions and corrections for its use, which, however, do not guarantee an accurate determination of the this specified mechanical characteristic for a specimen of increased flexibility. This drawback of the standard can be eliminated by using a nonlinear model that allows to obtain an exact solution to the problem of bending the DCB specimen.

Another problem is related to the deformation properties of the layered composite matrix. A huge number of tests have been carried out on laminated composites with a brittle polymer matrix. In the literature, however, there are practically no publications on the study of interlaminar fracture toughness of a layered composite with an elastic-plastic matrix. Therefore, a purposeful study of the behavior of such composite is of great interest, especially for perspective types of layered composite material.

The above mentioned two relevant problems determine the purpose of this work.

1.2. Aim of the Thesis

The main goal of this work is research that is focused on the analysis and solution of two actual problems of fracture mechanics of layered composites:

1. Improvement of method of interlaminar fracture toughness measurement by using nonlinear DCB specimen, corresponding technology and software of test data processing.
2. Estimation of effect of plasticity on the process of interlaminar delamination propagation in the layered composite of the elastic-plastic material of a matrix.

1.3. Tasks of the Thesis

1. Literature analysis of composite materials, testing methods and standards, as well as research of tests performed so far.

2. Analysis of the effect of DCB specimen non-linearity om the interlaminar fracture toughness measurement.
3. Theoretical model of the interlaminar fracture toughness for mixed I/II mode, based on the nonlinear theory of flexible plates.
4. Development of mathematical model of non-linear DCB specimen for the interlaminar fracture toughness measurement.
5. Experimental study of the interlaminar fracture toughness measurement of layered composite of high flexibility using the DCB specimen: material selection, specimen designing and manufacturing technology, procedure of testing.
6. Algorithm and MATLAB software of test results processing using non-linear DCB specimen.
7. Experimental study: effect of plasticity on the process of interlaminar delamination propagation in the layered composite of the elastic-plastic material of a matrix.
8. Processing of test results and extraction of main features on the effect of plasticity on the interlaminar fracture toughness of layered composite.

1.4. Scientific novelty

1. Analysis of the effect of DCB specimen non-linearity on the interlaminar fracture toughness measurement.
2. Development of theoretical model of the interlaminar fracture toughness for mixed I/II mode, based on the nonlinear theory of flexible plates.
3. Development of a mathematical model of non-linear DCB samples for the interlaminar fracture toughness measurement using nonlinear theory of flexible beam bending.
4. It was established that formally defined mode-I interlaminar fracture toughness is not a material constant and monotonically decreases as a function of delamination length.
5. It has been found that at constant extension rate the relationships between strain energy release rate, load and rate of delamination growth in the elastoplastic stage of loading are complex and mutually disproportionate.
6. Experimental results have been evaluated.

1.5. Practical significance

1. The use of a nonlinear model of the DCB specimen and the corresponding program MATLAB code allows to directly obtain the experimental value of the interlaminar fracture toughness of a layered material of low rigidity (low thickness or low modulus of elasticity of the composite).
2. The DCB model of the specimen and the corresponding program MATLAB code can also be useful in assessing the interlaminar fracture toughness that is obtained

from the linear DCB model and the nonlinearity corrections proposed by the standard.

3. The effects of the elastic-plastic properties of the matrix of the layered composite revealed during the tests and a thorough analysis of their results require a significant correction of the procedures for the calculated assessment of the interlaminar fracture toughness of the layered composite with the elastic-plastic properties of the matrix.

1.6. Methods of the research

1. Theory of elasticity of anisotropic materials.
2. Layered composites mechanics.
3. Strength theory of layered composites.
4. Non-linear theory of bending of flexible beams.
5. Fracture mechanics.
6. Experimental fracture mechanics.
7. Mathematic statistics.

1.7. Main results

1. Development of theoretical model of the interlaminar fracture toughness for mixed I/II mode, based on the nonlinear theory of flexible plates.
2. Development of mathematical model of non-linear DCB samples for the interlaminar fracture toughness measurement has been developed using nonlinear theory of flexible beam bending.
3. Algorithm and MATLAB software of test results processing using non-linear DCB specimen was created.
4. Satisfactory result can be obtained by using an equation that implies correction of the formal expression of G_{Ic} according to the linear model by its multiplication by the standard correction factor.
5. Results confirm the suitability of the nonlinear model of DCB specimen for determination of the G_{Ic} quantity of a composite within the limits of applicability of the standard test methods based on the Euler theory of bending of beams.
6. Experimental study on the effect of plasticity on the process of interlaminar delamination propagation in the layered composite of the elastic-plastic material of a matrix has been performed.

1.8. Composition and volume

The Thesis contains introduction, 5 chapters, conclusions, and references. The Thesis comprises 99 printed pages, 61 figures, 3 tables and bibliography containing 108 titles.

1.9. Approbation and publications

During the Thesis development 2 papers were published in international journals and 3 papers were published in conference proceedings.

Scientific publications

1. Pavelko V., Lapsa K., Pavlovskis P. The Effect of Plasticity to Interlaminar Fracture Toughness of Adhesive Bond of Composite. IOP Conference Series: Materials Science and Engineering, 2017, Vol. 251: 3rd International Conference on Innovative Materials, Structures and Technologies (IMST 2017), pp. 012081–012081. ISSN 1757-8981. e-ISSN 1757-899X. Available: doi:10.1088/1757-899X/251/1/012081
2. Pavelko V., Lapsa K., Pavlovskis P. Determination of the Mode I Interlaminar Fracture Toughness by using a Nonlinear Double-Cantilever Beam Specimen. Mechanics of Composite Materials, 2016, Vol.52, No.3, pp. 347–358. ISSN 0191-5665. e-ISSN 1573-8922. Available: doi:10.1007/s11029-016-9587-y

Conferences papers

1. Pavelko V., Kuzņecovs S., Lapsa K., Pavlovskis P. The Effect of Plasticity to Interlaminar Fracture Toughness of Adhesive Bond of Composite. In: Матеріали XIII міжнародної науково-технічної конференції "AВIA-2017", Ukraina, Kiev, April 19–21, 2017. Kiev: 2017, pp. 17.38–17.43.
2. Pavelko V., Lapsa K., Pavlovskis P. The Effect of Plasticity to Interlaminar Fracture Toughness of Adhesive Bond of Composite. In: 3rd International Conference "Innovative Materials, Structures and Technologies: (Abstracts), Latvia, Riga, September 27–29, 2017. Riga: RTU Press, 2017, p. 126.
3. Pavelko V., Lapsa K., Pavlovskis P. Определение вязкости межслойного разрушения первой моды с помощью нелинейного двухконсольного балочного образца. Механика композитных материалов = Mechanics of Composite Materials, 2016, Vol. 52, No. 3, pp. 491–506. ISSN 0203-1272

2 STRUCTURE OF THE THESIS

1. General overview of composite materials, testing and parameters that affect the performance of bonded joints

2. Research of interlaminar delamination of layered composites

3. Experimental part

4. Modelling of algorithm and MATLAB

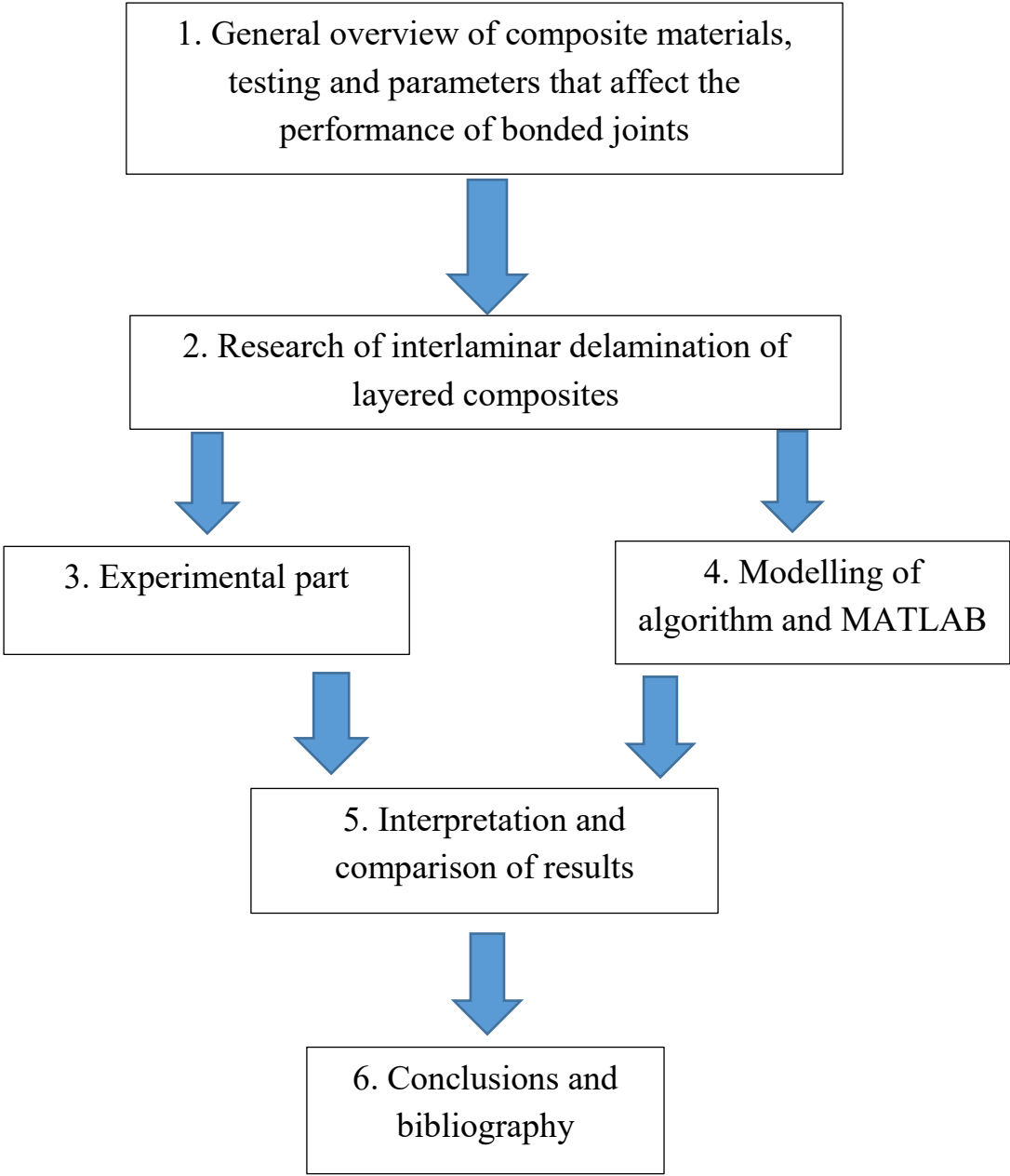5. Interpretation and comparison of results

6. Conclusions and bibliography

Fig. 2.1. Flowchart of the Thesis structure.

3. CONTENT OF THE THESIS

In Chapter 1, a general overview of the composite material and structures is described. The chapter explores the information about composite structures, manufacturing methods, properties, different failure types and testing.

In Chapter 2, a theoretical background of interlaminar fracture toughness is given. Also, more details are given on Mode I testing methodology. It also explores the MBT method. The chapter starts with some real-life examples of delamination and its causation.

The ASTM plots the delamination length normalized to the specimen thickness, a / h, as a function of the function of the matching cube root $C^{1/3}$, as shown in Fig. 3.1 [1].
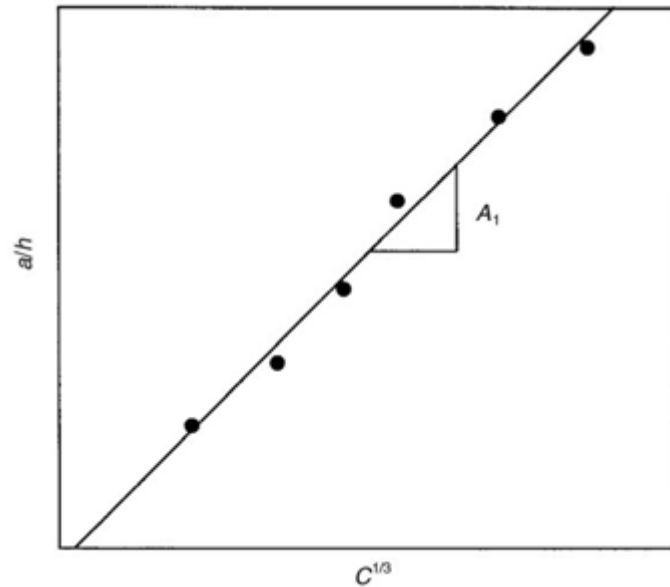

Fig. 3.1. Modified compliance calibration [1].

The ESIS approach is similar, but uses a slightly different nomenclature for thickness, where h is half the thickness of the laminate. The ESIS protocol recommends designing a product cube root with a width and fit (BC) of 1/3 of the thickness normalized delamination length, $a / 2h$. The slope of the least squares of this line gives the coefficient, m. The fracture toughness of Mode I interlayers is shown by Equation (3.1):

$$G_{Ic} = \frac{3m}{4h}\left(\frac{P}{B}\right)^2 (BC)^{2/3}, \tag{3.1}$$

Note that the ESIS protocol mistakenly refers to plotting $(BC)^{2/3}$ in the text and omits a factor of $2h$ in the equation for G_{Ic} [1].

Large displacement effects shall be corrected by the inclusion of a parameter, F, in the calculation of G_I:

$$F = 1 - \frac{3}{10}\left(\frac{\delta}{a}\right)^2 - \frac{3}{2}\left(\frac{\delta t}{a^2}\right), \tag{3.2}$$

where t is shown in Equation (3.2) for piano hinges.

This parameter F forms both the torque lever communication and the tilt of the end blocks. For samples with loading blocks, the distance from the end of the insert to the load line must be at least 50 mm so that the effect of the blocks is not taken into account. If not, the second parameter N must also be included, the displacement correction to take the stiffness of the specimen with blocks [2]:

$$N = 1 - \left(\frac{L'}{a}\right)^3 - \frac{9}{8}\left[1 - \left(\frac{L'}{a}\right)^2\right]\left(\frac{\delta t}{a^2}\right) - \frac{9}{35}\left(\frac{\delta}{a}\right)^2, \qquad (3.3)$$

where t and L' are shown in Equation (3.3) for end blocks [2].

The determination of interlaminar fracture toughness for a mixed mode is governed by the ASTM D 6671-01 standard, which is based on linear theory of plate and has several significant limitations related to the requirements for the characteristics of the specimen. This paragraph discusses an alternative option for determining the interlaminar fracture toughness for mixed loading mode based on the nonlinear theory of flexible plates [3], [4].

A layered elastic composite plate of thickness h contains a number of horizontal layers whose principal axes of elasticity coincident with axes x, y of Cartesian references system (Fig. 3.2).

Global compressive strain of the plate between tip cross-sections of part of a plate under delamination is equal to ε and defined by axial relative displacement between those cross-sections Δl (Fig. 3.2). So

$$\varepsilon \approx \frac{\Delta l}{l}. \qquad (3.4)$$

It is assumed that

$$\varepsilon > \varepsilon_{cr},$$

where ε_{cr} is the axial strain of sub-layer at critical force of buckling. We can see that

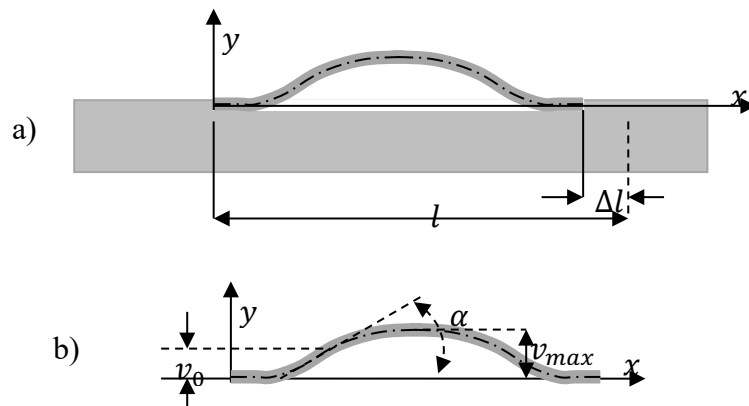$$\varepsilon_{cr} = \frac{\pi^2 t^2}{3l^2}. \qquad (3.5)$$

Fig. 3.2. A layered composite plate (a) with delamination and (b) the geometrical parameters of sub-layer.

The global longitudinal strain of sub-layer at the base l consists of two components: ε_c is related with action of compressive axial force (the compression strain) and ε_b is related with action of bending moment (bending strain):

$$\varepsilon = \varepsilon_c + \varepsilon_b. \tag{3.6}$$

The middle cylindrical surface of sub-layer has a generatrix which can be described by an exact differential equation of bending theory of flexible plate:

$$D\frac{d\theta}{ds} = M(x) = M_0 - Pv(x), \tag{3.7}$$

where
D – cylindrical stiffness of sub-layer;
s – length of the generatrix of cylindrical surface;
$d\theta/ds$ – curvature of the generatrix;
$M(x)$ – bending moment in equation (3.7), expressed in terms of its value M_0 at the source of cartesian references system and the compressive force P in the cross-section;
$v(x)$ – sub-layer deflection.

Equation (3.7) can be transformed to the differential equation in natural form:

$$\frac{d\theta}{ds} = k\sqrt{2(\cos\theta - \cos\alpha)}, \tag{3.8}$$

where

$$\cos\alpha = 1 - \frac{M_0^2}{2DP} \quad and \quad k = \sqrt{\frac{P}{D}}$$

and α is the maximum angle of the tangent of the generatrix of cylindrical surface of the sub-layer. This angle corresponds to the point of zero-curvature shown in Fig. 3.2 b.
k is defined by the compressive force and cylindrical stiffness of sub-layer.

It can be seen that

$$k = \sqrt{\frac{P}{D}} = \frac{2\pi}{l}\sqrt{\bar{P}}, \tag{3.9}$$

where

$$\bar{P} = \frac{P}{P_{cr}}$$

and the critical force

$$P_{cr} = \frac{4\pi^2 D}{l^2}.$$

13

The strain energy related with the action of axial compressive force N (simply, compression energy):

$$U_c = \int_0^l \frac{N^2}{2E^*t}\,ds = \int_0^l \frac{(P\cos\theta)^2}{2E^*t}\,ds. \tag{3.10}$$

After integration and transformations,

$$U_c = \frac{1}{6}\frac{P^2l}{E^*t}\frac{[(4p^2-1)K(p^2)+4(1-2p^2)E(p^2)]}{K(p^2)}. \tag{3.11}$$

In compact forms the compression energy is showed in Equation (3.12):

$$U_c = \frac{1}{2}E^*lt\bar{P}\varepsilon_{cr}\varepsilon_c = \frac{1}{2}E^*lt\bar{P}\varepsilon_{cr}^2\bar{\varepsilon}_c. \tag{3.12}$$

In the above equations, E is the elasticity modulus and v is the Poisson's ratio of a sub-layer material and the elasticity modulus of plane strain state:

$$E^* = \frac{E}{1-v^2}.$$

.

The strain energy connected with bending of the sub-layer (simply, bending energy):

$$U_b = \int_0^l \frac{M^2}{2D}\,ds = \frac{D}{2}\int_0^l \left(\frac{d\theta}{ds}\right)^2\,ds, \tag{3.13}$$

but in terms of the complete elliptic integrals

$$U_b = \frac{1}{2}E^*tl4[(p^2-1)K(p^2)+E(p^2)]\bar{P}\varepsilon_{cr}. \tag{3.14}$$

The compact form of a bending energy:

$$U_b = \frac{1}{2}E^*tl2(\varepsilon_\alpha - \varepsilon_b)\bar{P}\varepsilon_{cr}, \tag{3.15}$$

where $\varepsilon_\alpha = 1 - \cos\alpha = 2p^2$ can be interpreted as the superior limit of the longitudinal deformation due to bending.

The strain energy of the plate part with delamination is as follows:

$$U = U_0 - U_c - U_b, \tag{3.16}$$

where U_0 is strain energy with closed delamination:

$$U_0 = \frac{1}{2}E^*lt\varepsilon^2. \tag{3.17}$$

Using Equations (3.12), (3.14), and (3.16) the strain energy released by buckling of a sub-layer can be represented as follows:

$$U = \frac{1}{2}E^*lt\left[\varepsilon^2 - \bar{P}\varepsilon_{cr}[\varepsilon - \varepsilon_b + 2(\varepsilon_\alpha - \varepsilon_b)]\right]. \tag{3.18}$$

At virtual extending of delamination, the total strain energy release rate G is:

$$G = \frac{dU}{tdl} = \frac{1}{2}E^*\left\{\varepsilon^2 + \varepsilon_{cr}\bar{P}[\varepsilon - \varepsilon_b + 2(\varepsilon_\alpha - \varepsilon_b)] - \varepsilon_{cr}\frac{d}{dl}\left[\bar{P}[\varepsilon_c + 2(\varepsilon_\alpha - \varepsilon_b)]\right]\right\}, \quad (3.19)$$

and finally,

$$G = \frac{dU}{tdl} = \frac{1}{2}Et(\varepsilon^2 + a_1\varepsilon_{cr}\varepsilon + a_2\varepsilon_{cr}), \quad (3.20)$$

where $a_1 = \bar{P}$ and

$$a_2 = \bar{P}\left\{2\varepsilon_\alpha - 3\varepsilon_b - 2\left[3\frac{E'(p^2)K(p^2) - E(p^2)K'(p^2)}{K^2(p^2)} + 2\right]\frac{2\varepsilon_{cr}\bar{\varepsilon}_c}{\varepsilon_{cr}\bar{\varepsilon}_c' + \varepsilon_b'}\right\}.$$

Equation (3.20) is the second order polynomial of the total longitudinal strain ε depending on the critical strain ε_{cr} and parameter p^2 of the buckled shape of sub-layer.

The condition of delamination propagation is:

$$G = G_c, \quad (3.21)$$

where G_c is the critical strain energy release rate postulated as a material constant on mixed I/II modes.

Using Equations (3.15) and (3.16) this condition can be presented as follows:

$$\varepsilon^2 + a_1\varepsilon_{cr}\varepsilon + a_2\varepsilon_{cr} = \varepsilon_0^2 , \quad (3.22)$$

where

$$\varepsilon_0^2 = \frac{2tG_c}{E^*}. \quad (3.23)$$

It is evident that the strain energy release rate in Equation (3.19) is a function of three variables: the total relative strain ε , the l/t ratio of the sub-layer, and the parameter p^2 of buckled shape. Therefore, to determine the critical configuration of the buckled sub-layer, the following algorithm should be realized [3]:

$$(\varepsilon_{cr}\bar{\varepsilon}_c + \varepsilon_b)^2 + a_1\varepsilon_{cr}(\varepsilon_{cr}\bar{\varepsilon}_c + \varepsilon_b) + a_{21}\varepsilon_{cr} + a_{22}\varepsilon_{cr}^2 = \varepsilon_0^2, \quad (3.24)$$

where

$$a_{21} = \bar{P}(2\varepsilon_\alpha - 3\varepsilon_b);$$

$$a_{22} = \bar{P}\left\{-2\left[3\frac{E'(p^2)K(p^2) - E(p^2)K'(p^2)}{K^2(p^2)} + 2\right]\frac{2\bar{\varepsilon}_c}{\varepsilon_{cr}\bar{\varepsilon}_c' + \varepsilon_b'}\right\}.$$

As coefficient a_{22} depends on the critical strain ε_{cr}, this algorithm requires iteration procedure.

15

The pre-condition of successful test for measurement of the interlaminar fracture toughness of a mixed II/I mode using the specimen with thin delamination is sufficient strength of sub-layer at compression/banding combined load for which the strength is defined by ultimate strain ε_u. The problem of strength of sub-layer was considered in [3] and [4].

In the study done by V. Pavelko [3] in Fig. 3.3 there is a graph showing the behavior of the compressed sub-layer with a gradual increase of total deformation for $\varepsilon_u/\varepsilon_0 = 1$ and $\varepsilon_0 = 7.8 \cdot 10^{-3}$. First of all, if the compressive strength of the plate and the sub-layer is the same, then for small values of the ratio $\bar{l} = l/t$ the destruction of the plate happens until buckling of sub-layer. In all cases, below the critical strain (dash-dotted line) the sub-layer does not buckle. In the region above this line but below the combined solid line delamination is not propagated, and there is no destruction. If the total deformation of the composite reaches a value corresponding to the combined bold line, there are two possible scenarios of the damage behavior. If the ratio length/thickness of the sub-layer is not more than $\bar{l}_*$ (equal to 72 in this case), the maximum compressive strain in a dangerous cross-section of the sub- layer reaches the limit ε_u and the sub-layer collapse [3].

If the ratio length/thickness of the sub-layer is not more than $\bar{l}_*$ (equal to 72 in this case), the maximum compressive strain in a dangerous cross-section of the sub-laminate reaches the limit ε_u and the sub-laminate collapse. If the length/thickness ratio is more than $\bar{l}_*$, then the stable propagation of delamination can be observed. If the total strain reaches ε_0, then the breakaway of sub-layer occurs along the entire length of the composite [3].
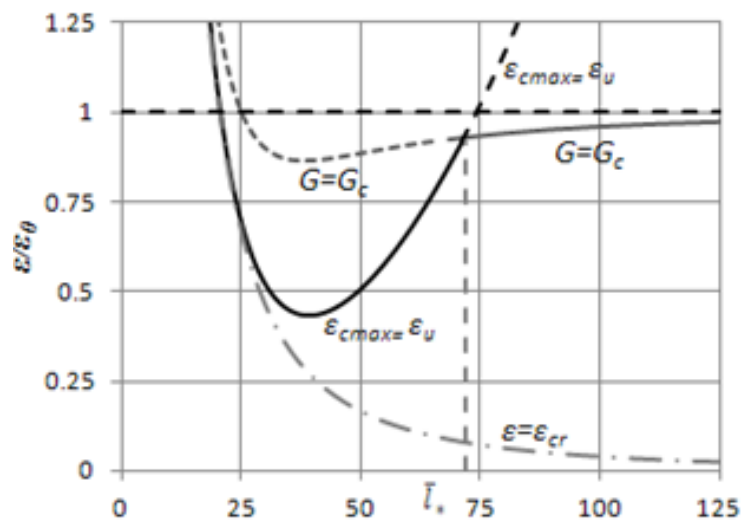

Fig. 3.3 Sub-layer destruction-delamination propagation curves [3].

Results of calculation of the delamination propagation and the strength curves are presented in Fig. 3.4 for different $\varepsilon_u/\varepsilon_0$ relations [3].
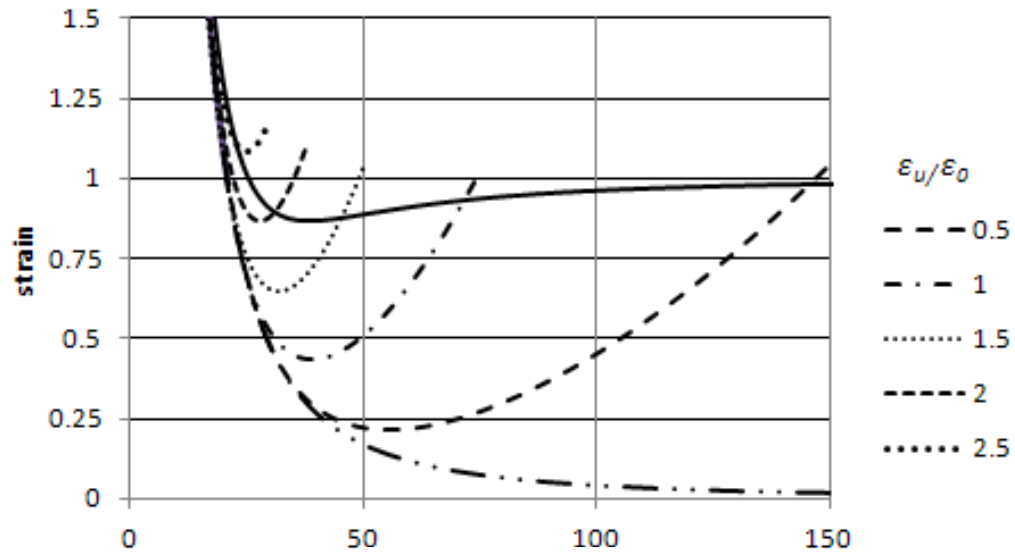
16

Fig. 3.4. Delamination propagation and strength curves [3].

Final conclusions:

1. The specimen with thin delamination is potentially useful for measurement of the interlaminar fracture toughness of layered composite: there is always the length/thickness interval for which the stable growth of delamination can be realized.

2. Equation (3.22) can be used for the processing of test data and defining of the interlaminar fracture toughness of mixed II/I mode.

3. Relation between G_I and G_{II} can be obtained by using corresponding components of the strain energy.

4. It makes sense to continue problem investigation including lab tests.

In Chapter 3, represents analytical model of nonlinear DCB specimen for determination of the Mode I Interlaminar fracture toughness. Specimens in a form of DCB are most widely used in the practice of experimental determination of the interlaminar fracture toughness of layered composites for the I, II, and mixed I/II fracture modes. The dependence of R-curves on the geometry of DCB samples for a unidirectional epoxy-carbon composite has been investigated [5].

It is obvious that the nonlinear bending theories of flexible beams are promising for perfection of the method of determination of G_{Ic} for layered composites on the basis of DCB specimens (Fig. 3.5) if the theory of elastic flexible plates with large displacements is used [6].
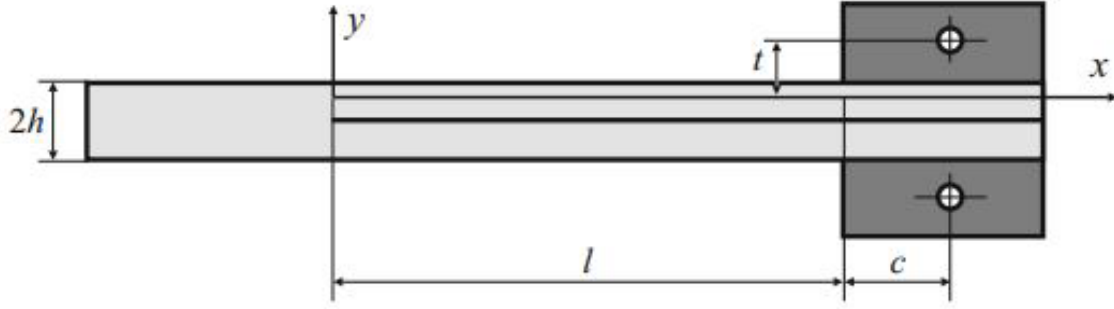
17

Fig. 3.5. Scheme and main dimensions of a DCB specimen [6].

Usually, the width of the cross section of a specimen is much greater than its height ($b \gg h$); therefore, it can be assumed that the specimen is in a stress state close to the plane one. Thus, the differential equation of the deflection curve of a beam can be written as Equation (3.25) of a plane curve in the natural form:

$$D \frac{d\theta}{ds} = M(s), \tag{3.25}$$

where θ is the rotation angle of the cross section of the beam with a curvilinear coordinate s, $M(s)$ is the bending moment in this section, and D is the cylindrical rigidity of the beam.

The bending moment can be expressed in terms of its value M_0 in the root cross section, the external active force P, and the axial displacement $u(s)$ in the cross section s:

$$M(s) = M_o - P[s - u(s)].$$

After insertion of this expression into Equation (3.25) and simple transformations, the differential equation of the deflection curve takes the form shown in Equation (3.26):

$$\frac{d\theta}{ds} = k\sqrt{2}\sqrt{\sin\alpha_0 - \sin\theta}, \tag{3.26}$$

where

$$\sin\alpha_0 = \sin\alpha + \frac{(kl)^2}{2}(\bar{c}\cos\alpha - \bar{t}\sin\alpha)^2,$$

$$\sin\alpha = \frac{1}{2}\left(\frac{M_0}{kD}\right)^2, k^2 = \frac{P}{D}, \bar{c} = \frac{c}{l}, \bar{t} = \frac{t}{l}.$$

Here, α is the rotation angle of the end section $s = l$ of the beam (see Fig. 3.5) and α_0 is the rotation angle in the cross section of the beam with a zero curvature of the deflection curve. For the configuration of the specimen at $c = t = 0$, the cross section of zero curvature coincides with the beam end $s_0 = l$. If $\bar{c}\cos\alpha - \bar{t}\sin\alpha > 0$, this section corresponds to a curvilinear coordinate $s_0 > l$, i.e. it does not exist in reality. In this case, the curvature of the beam is a positive decreasing function of coordinate s. But if $\bar{c}\cos\alpha - \bar{t}\sin\alpha < 0$, the curvilinear coordinate of the cross section of zero curvature $s_0 < l$, and this means that, upon transition through this section, the curvature changes its sign. It is obvious that the cross section with the zero curvature of the deflection curve coincides with the beam end on the condition that

18

$$\alpha = \alpha_* = \cotan(c/t). \tag{3.27}$$

If is fulfilled, then, as follows from Equation (3.26),

$$ds = \frac{d\theta}{k\sqrt{2}\sqrt{\sin\alpha_0 - \sin\theta}}.$$

If $\alpha < \alpha_0$, the rotation angle $\theta(s)$ grows monotonically. At $\alpha > \alpha_0$, the rotation angle θ grows in interval $[0, s_0]$ from *zero* to α_0 and then decreases in $[s_0, l]$ from α_0 to α. As a result, in the first case,

$$s = \int_0^s ds = \int_0^{\theta(s)} \frac{d\theta}{k\sqrt{2}\sqrt{\sin\alpha_0 - \sin\theta}}$$

and in the second one,

$$s = \begin{cases} \int_0^{\theta(s)} \dfrac{d\theta}{k\sqrt{2}\sqrt{\sin\alpha_0 - \sin\theta}} & at\ s \le s_0 \\[2ex] \int_0^{a_0} \dfrac{d\theta}{k\sqrt{2}\sqrt{\sin\alpha_0 - \sin\theta}} + \int_\theta^{a_0} \dfrac{d\theta}{k\sqrt{2}\sqrt{\sin\alpha_0 - \sin\theta}} & at\ s \le s_0 \end{cases}.$$

Calculations by these equations for the variable limit of integration $\theta(l) = \alpha$ make it possible to derive the dimensionless parameter kl of the external load as a function of the rotation angle α of the end section of the deformed part of the beam, as follows in Equation (3.28):

$$kl = \frac{1}{\sqrt{2}} \begin{cases} I_l(0, \alpha) & at\ \alpha \le \alpha_* \\ I_l(0, \alpha_0) + I_l(\alpha, \alpha_0) & at\ \alpha \le \alpha_*, \end{cases} \tag{3.28}$$

where

$$I_l(\alpha_1, \alpha_2) = \int_{\alpha_1}^{\alpha_2} \frac{d\theta}{\sqrt{\sin\alpha_0 - \sin\theta}}.$$

It is seen that the dimensionless parameter kl is uniquely related to the rotation angle α. The deflection curve of the beam can also be described in rectangular coordinates shown in Equations (3.29) and (3.30):

$$x(\theta) = \frac{1}{k\sqrt{2}} \int_0^\theta \frac{\cos\theta d\theta}{\sqrt{\sin\alpha_0 - \sin\theta}}, \tag{3.29}$$

$$y(\theta) = \frac{1}{k\sqrt{2}} \int_0^\theta \frac{\cos\theta d\theta}{\sqrt{\sin\alpha_0 - \sin\theta}}. \tag{3.30}$$

It is obvious that ordinate $y(\theta)$ coincides with deflection of the beam, $v(\theta)$. Equation (3.5) is simply integrated and takes the form as in Equation (3.31):

$$\bar{x}(\theta) = \frac{x(\theta)}{l} = \begin{cases} \dfrac{\sqrt{2}}{kl}\left(\sqrt{\sin\alpha_0} - \sqrt{\sin\alpha_0 - \sin\theta}\right) & at\ s < s_0, \\[2ex] \dfrac{\sqrt{2}}{kl}\left(\sqrt{\sin\alpha_0} + \sqrt{\sin\alpha_0 - \sin\theta}\right) & at\ s > s_0 \end{cases}. \tag{3.31}$$

19

The deflection in Equation (3.30) can be conveniently expressed in terms of integrals $I_1(\alpha_1, \alpha_2)$ and $I_2(\alpha_1, \alpha_2)$ in Equation (3.32):

$$\bar{v}(\theta) = \frac{v(\theta)}{l} = \frac{1}{kl\sqrt{2}} \begin{cases} -l_2(0,\theta) + \sin\alpha_0 I_l(0,\theta) \text{ at } s < s_0 \\ -l_2(0,\alpha_0) + \sin\alpha_0 I_l(0,\alpha_0) - \\ -l_2(\theta,\alpha_0) + \sin\alpha_0 I_l(\theta,\alpha_0) \text{ at } s > s_0 \end{cases}, \qquad (3.32)$$

where

$$l_2(\alpha_1, \alpha_2) = \int_{\alpha_1}^{\alpha_2} \sqrt{\sin\alpha_0 - \sin\theta}\, d\theta.$$

As seen from Equations (3.28), (3.31), and (3.32), the geometrical form of the deflection curve of a cantilever beam is also uniquely determined by the rotation angle of its end section [6].

If we assume that the effect of shear force on the elastic strain energy is weaker, then, at large deflections of the cantilever, this energy depends on two internal force factors: the bending moment and axial force. In what follows, the corresponding components of strain energy will be called the bending energy and the tension energy [6].

The bending energy of the cantilever can be presented in finite form as shown in Equation (3.33):

$$U_b = \int_0^l \frac{M^2}{2D}\, ds = \frac{kD}{\sqrt{2}} \begin{cases} I_2(0,\alpha) \text{ at } \alpha < \alpha_* \\ I_2(0,\alpha_0) + I_2(\alpha,\alpha_0) \text{ at } \alpha < \alpha_* \end{cases}. \qquad (3.33)$$

The tension energy is determined by the axial tensile force $N = P\sin\alpha$, which is projection of the external active force on the direction of tangent to the deflection curve of the beam, as shown in Equation (3.34):

$$U_t = \int_0^l \frac{N^2}{2Eh}\, ds. \qquad (3.34)$$

After simple transformations, we have Equation (3.35):

$$U_t = \frac{D(kl)^4}{72h\bar{l}^3} \begin{cases} I_1(\alpha_0) + \sin\propto \alpha_0 I_2(0,\alpha) \text{ at } \alpha < \alpha_* \\ I_2(\alpha_0) + \sin\alpha_0 [I_2(0,\alpha_0) + I_2(\alpha,\alpha_0)] \text{ at } \alpha > \alpha_* \end{cases}. \qquad (3.35)$$

In a dimensionless form, the components of strain energy read as in Equations (3.36) and (3.37):

$$\bar{U}_b = \frac{U_b}{D/h} = \frac{kl}{\bar{l}\sqrt{2}} \begin{cases} I_2(0,\alpha) \text{ at } \alpha < \alpha \propto_* \\ I_2(0,\alpha_0) + I_2(\alpha,\alpha_0) \text{ at } \alpha < \alpha_* \end{cases}, \qquad (3.36)$$

$$\bar{U}_t = \frac{U_t}{D/h} = \frac{(kl)^4}{72\bar{l}^3} \begin{cases} I_1(\alpha_0) + \sin\alpha \propto_0 I_2(0,\alpha) \text{ at } \alpha < \alpha_* \\ I_2(\propto \alpha_0) + \sin\alpha_0 [I_2(0,\alpha_0) + I_2(\alpha,\alpha_0)] \text{ at } \alpha > \alpha_* \end{cases}, \qquad (3.37)$$

where $\bar{l} = l/h$,

$$I_1(\alpha_0) = 2 - \cos 2\alpha_0 - \frac{\sqrt{2}}{kl}(\sqrt{\sin\alpha_0} - \cos\alpha\sqrt{\sin\alpha_0 - \sin\alpha}),$$

$$I_2(\alpha_0) = 2 - \cos 2\alpha_0 - \frac{\sqrt{2}}{kl}(\sqrt{\sin\alpha_0} - \cos\alpha\sqrt{\sin\alpha_0 - \sin\alpha}),$$

and the total strain energy of the DCB specimen is shown in Equation (3.38):

$$\bar{U} = 2(\bar{U}_b + \bar{U}_t). \tag{3.38}$$

If $\alpha \le \alpha_*$, the integrals, $I_1(\alpha_1,\alpha_2)$ and $I_2(\alpha_1,\alpha_2)$, are improper, and their numerical calculation requires a constant control of accuracy. This can be avoided by employing the transformation of the variable θ determined according to Equation (3.39):

$$\sin\left[\frac{1}{2}\left(\theta + \frac{\pi}{2}\right)\right] = p\sin\varphi, \tag{3.39}$$

where

$$p = \sin\left[\frac{1}{2}\left(\alpha_0 + \frac{\pi}{2}\right)\right].$$

As a result, the integrals mentioned turn into the incomplete elliptic integrals of the first and second kind, $F(\varphi_0, \varphi_*, p^2)$ and $E(\varphi_0, \varphi_*, p^2)$, respectively:

$$l_1(\alpha_1, \alpha_2) = \frac{1}{\sqrt{2}}F(\varphi_0, \varphi_*, p^2),$$

$$l_2(\alpha_1, \alpha_2) = 2\sqrt{2}[(p^2 - 1)F(\varphi_0, \varphi_*, p^2) + E(\varphi_0, \varphi_*, p^2)],$$

where

$$F(\varphi_0, \varphi_*, p^2) = \int_{\varphi_0}^{\varphi_*} \frac{d\varphi}{\sqrt{1 - p^2\sin\varphi}},$$

$$E(\varphi_0, \varphi_*, p^2) = \int_{\varphi_0}^{\varphi_*} \sqrt{1 - p^2\sin\varphi}\, d\varphi.$$

The limits of integration are determined by the basic transformation in Equation (3.39):

$$\sin\varphi_i = \frac{\sin\left(\frac{a_i}{2} + \frac{\pi}{4}\right)}{\sin\left(\frac{a_0}{2} + \frac{\pi}{4}\right)}.$$

According to the definition, energy release rate G_I for a DCB specimen:

$$G_I = -\frac{dU}{dl} = -\frac{D}{h^2}\frac{d\bar{U}}{d\bar{l}} = \frac{D}{h^2}\bar{G}. \tag{3.40}$$

In the particular case where the external force is applied to the end of the cantilever $(c = t = 0)$, an accurate, but rather complex, formula for estimating the energy release rate of a DCB specimen can be obtained. Therefore, for practical applications, it is more convenient to use a numerical differentiation. In this case, it is necessary to bear in mind that the derivative of strain energy along the crack length has to be calculated at a constant opening of delamination.

It is obvious that, in testing a DCB specimen with controlled displacements in the state of critical equilibrium, the energy release rate is equal to the interlaminar fracture toughness. The initial data for determining quantity G_{Ic} are the critical force P_c, the corresponding opening δ (relative displacement of the points of application of external forces), and the delamination length l_c at the instant of its next jump-like growth. These are the parameters measured in standard tests [7], [8] that are redundant. Therefore, there are several variants of determination of parameter G_{Ic} according to test data, which allow one to control the final result. In the present study, the determination of G_{Ic} according to the nonlinear model of DCB specimens implies an iterative procedure employing the opening and length of delamination.

The algorithm for determining the strain energy, its release rate upon propagation of delamination, and the toughness G_{Ic} according to the nonlinear model of DCB specimen, was realized in the form of a MATLAB program code [7].

In Chapter 4, in [8], the suitability of the developed nonlinear model of DCB specimen was verified by comparing its predictions with the test data for specimens of a layered fiberglass within the limits of applicability of the standard [2], [9]. A practically exact coincidence between the results obtained by the nonlinear model and standard method of MBT was observed. However, the question of adequacy of the nonlinear model outside the limits of applicability of the standard methods remains open. To make up for the deficiency, DCB specimens of increased flexibility were tested. We used a layered CFRP based on carbon fabric 200 g/m² as the reinforced material and an epoxy resin as the binder. The specimens were manufactured by the vacuum technology with cure for 24 h at a temperature of 28 °C [5].

A 10-layer specimen had a total thickness of 2 mm and dimensions 20.5 × 200 mm in the plan. The initial delamination between the fifth and sixth layers was created by a teflon interlayer in the specimen structure. The DCB specimen was subjected to the action of a splitting load by means of piano hinges pasted to the ends of cantilevers, so that the axes of hinges were located in the end cross section of cantilevers shown in Fig. 3.6.
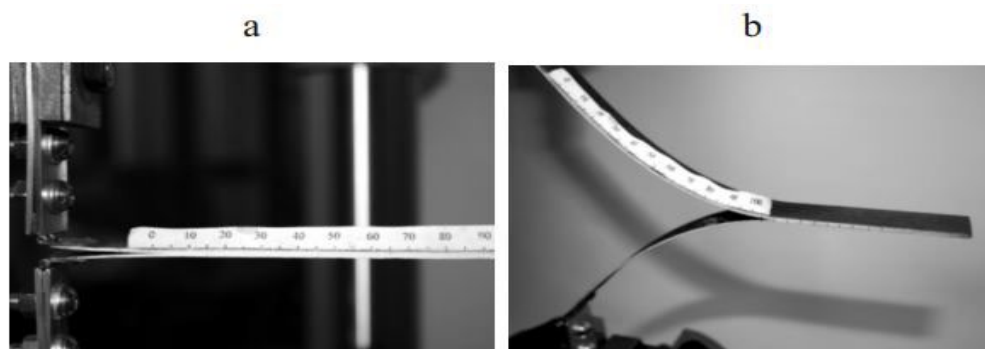

Fig. 3.6. Photos of a DCB specimen (a) at the initial stage of tests and (b) at a great opening of delamination [5].

The standard procedure for determination of the effective length of delamination, found by analyzing the elastic compliance of a specimen in relation to the delamination length (Fig. 3.7), was used.
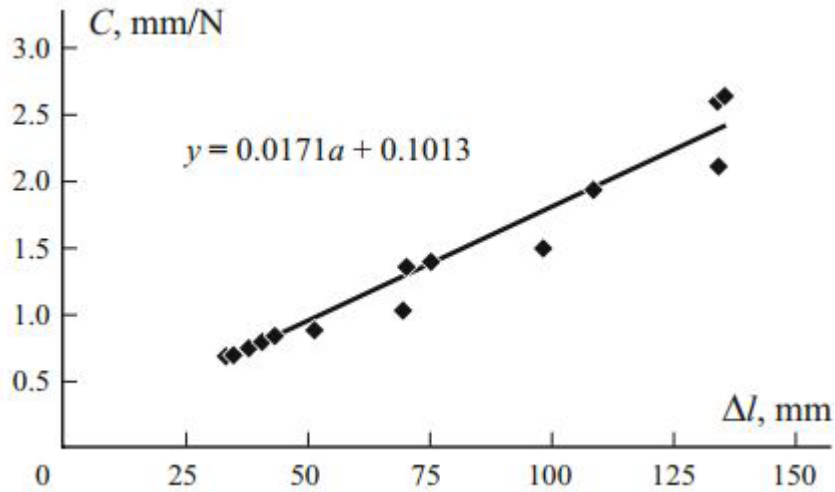

Fig. 3.7. Compliance C of a DCB specimen vs delamination length Δl [5].

The basic results of measurements and calculations of toughness G_{Ic} are presented in Table 3.1 [5].

Table 3.1

Values of Interlaminar Fracture Toughness According to Experimental Results [5]

a, mm	P_c, H	δ, mm	$\left(\frac{\delta}{a}, \frac{a}{t}\right)$	G_{Ic}, J/m²			
				Nonlinear model	MBT method	From P_c and α_e	According to linear model
33.4	36.2	14.7	0.91	999	1077	1062	969
34.4	36.4	16.3	0.90	1080	1178	1128	1017
37.8	32.3	17.6	0.91	954	1035	1045	948
40.3	31.3	20.4	0.89	1014	1113	1100	984
43.2	28.5	21.4	0.90	905	988	1029	927
51.1	26.0	33.6	0.84	1107	1278	1155	972
68.7	18.9	48.4	0.83	878	1035	1043	863
74.6	19.9	60.2	0.78	1059	1315	1346	1050
97.1	14.5	90.0	0.72	890	1192	1170	843
106.9	14.3	106.2	0.68	942	1328	1372	937
135.0	13.5	167.0	0.52	1080	1961	1898	988
147.0	12.5	190.0	0.48	1037	2041	1916	918
135.0	12.1	151.0	0.61	891	1412	1525	924
138.0	12.7	161.0	0.57	970	1619	1752	1003

Results of investigation confirm the suitability of the nonlinear model of DCB specimen for determination of the quantity G_{Ic} of a composite within the limits of applicability of the standard test methods based on the Euler theory of bending of beams. Figure 3.8 shows a comparison between the estimates obtained by the nonlinear model and the standard MBT method.
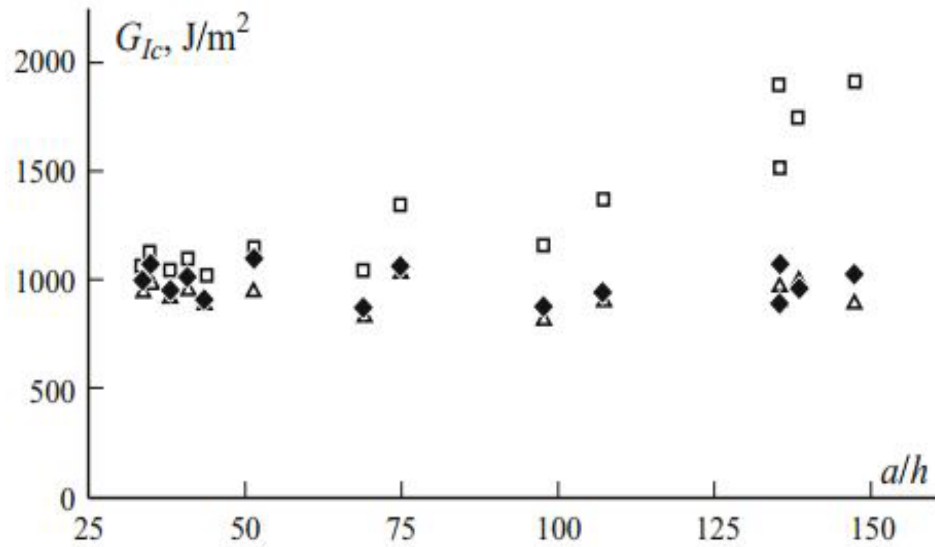

Fig. 3.8. Relation between G_{Ic} and the relative size of delamination a/h according to the nonlinear (♦) linear (□) and corrected (△) models of DCB specimen [5].

The second basic conclusion concerns the use of correction, which is recommended by the standard for considering changes in the arm of force at large deflections. As follows from the results of our investigations, the direct correction envisaged by the standard may even worsen the estimate of G_{Ic} if the MBT method is employed [5].

In Chapter 5, the results of investigation of the effect of plasticity to interlaminar fracture toughness of adhesive bond of composite are shown. The glass/epoxy laminate reinforced by glass fabric was used for preparation of the test samples. 25 × 125 mm strips were cut from the GFRP 2 mm thick plate and were used as the adherents of adhesive joint manufacturing in the form of the DCB specimen (Fig. 3.5) with initial deboning 55–60 mm [10].

During the test with the controlled displacement of 3 mm/min rate, the data force /extension (load points relative displacement) was digitally stored permanently with periodic stops for accurate fixing of the current size of delamination.

The curves of loading are shown in Figs. 3.9 and 3.10 for a specimen of Group 1 and Group 2, respectively. In the legend of the plot on the right side, the delamination initial length before each next step of loading is shown.
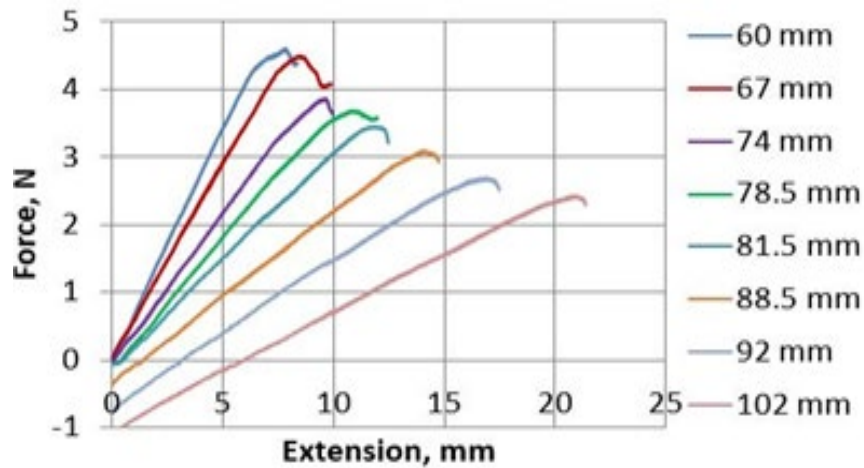
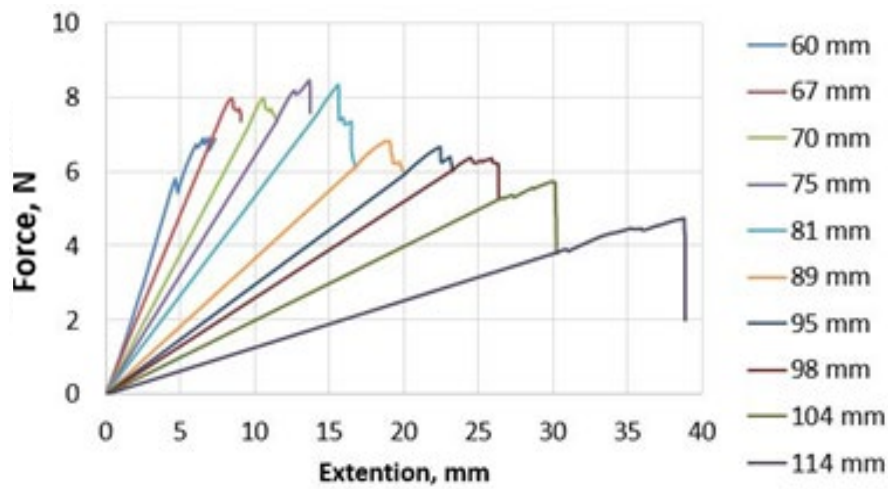Fig. 3.9. Force/extension function for a specimen of Group 1 [11].

Fig. 3.10. Force/extension function for a specimen of Group 2 [11].

In general, it can be concluded that the adhesive layer in the samples of Group 1 have pronounced elastoplastic properties. A specimen of Group 2 is characterized by an elastic behavior and brittle fracture of the adhesive layer (Fig. 3.11) [11].

In Fig. 3.11, the results of test data processing are presented for the samples of Group 1. Each point of this graph corresponds to the maximum of the experimental curve load/extension of the corresponding step of test. The length of delamination is estimated using the regression equation [11].
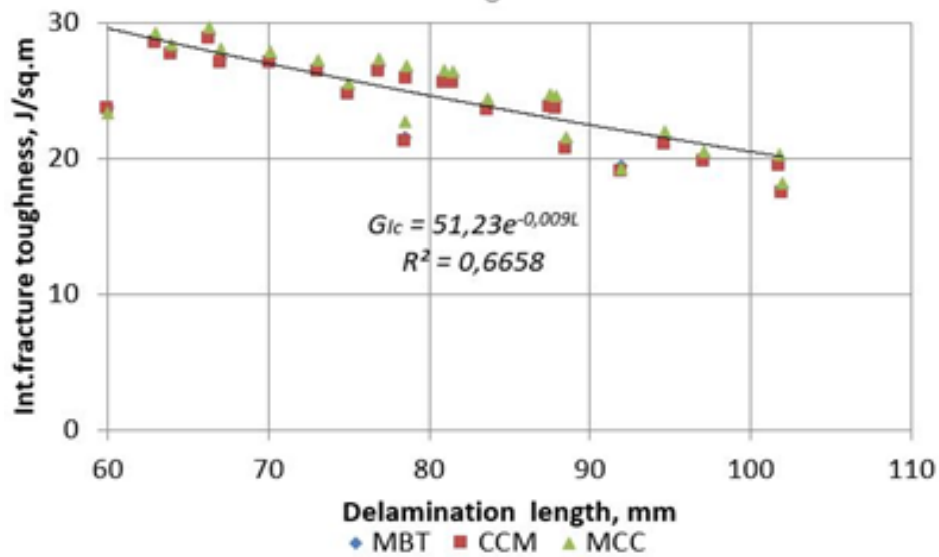
Fig. 3.11. Interlaminar fracture toughness as a function of delamination length of the Group 1 specimen [11].

It is seen that for the samples of Group 2 (Fig. 3.12) beginning from the 70 mm, delamination length G_{Ic} is constant about 150 J/m². Only for the initial length of delamination the G_{Ic} is smaller. Usually, this effect is called an R-curve [11].
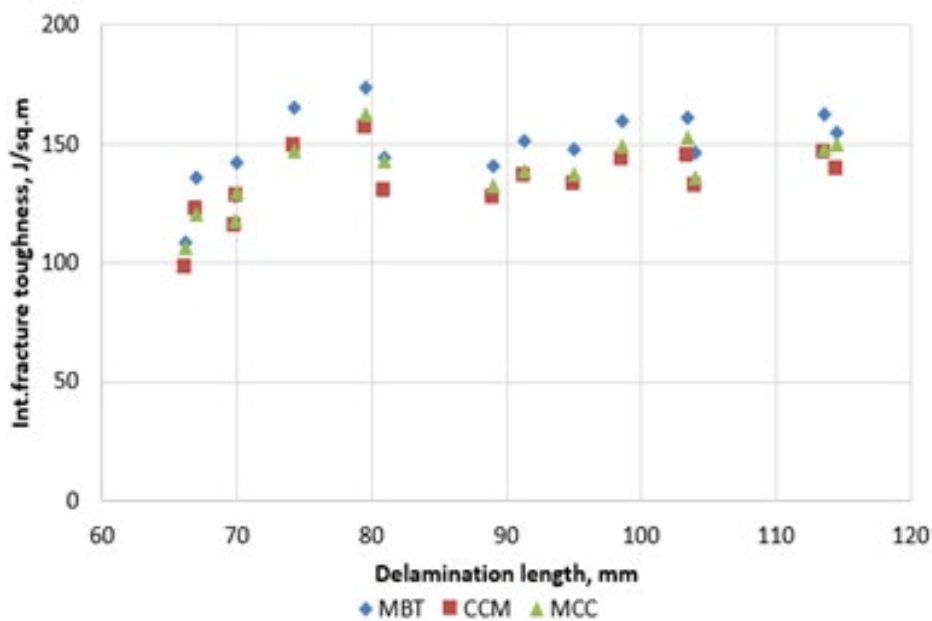

Fig. 3.12. Interlaminar fracture toughness as a function of delamination length of the Group 2 specimen [11].

For the samples of Group 1, this parameter is significantly lower, and the monotonic decrease is observed with the increase of delamination length [13].

Results of this research show that at elastic-plastic behavior of adhesive material there is specific continuous smooth growth of delamination without jump-like propagation that is observed for brittle material.

If the adhesive material is elastoplastic, then the process of progressive delamination is much more complicated. In the present study, the effect of plasticity on its interlaminar strength was investigated. A comparative analysis of the test data was carried out for two groups of samples from the same two-component adhesive material. For one of the groups the curing time was reduced in comparison with the standard. As a result, it became possible to assess the influence of technological faults to the strength of the adhesive joint. However, the main purpose of the analysis was to examine the patterns of delamination growth caused by plasticity of the adhesive material [13].

4. CONCLUSIONS

The presented results of research show that the main aims of the Thesis have been achieved. All planned analytical and experimental studies have been performed:

1. Literature analysis of composite materials, testing methods and standards, as well as research of tests performed so far showed that physico-chemical, mechanical, structural, and other properties of layered composites are defined as well as their advantages and also specific scientific, technical, technological, and operational problems.

2. Analysis of the effect of DCB specimen non-linearity on the interlaminar fracture toughness measurement were performed and showed that the existing standard methods of DCB specimen use for this purpose are approximate and there are a number of restrictions for use of these methods.

3. Development of mathematical model of non-linear DCB samples for the interlaminar fracture toughness measurement was developed using nonlinear theory of flexible beam bending.

4. Experimental study of the interlaminar fracture toughness measurement of layered composite of high flexibility using the DCB specimen (material selection, specimen designing and manufacturing technology, procedure of testing) was performed.

5. Algorithm and MATLAB software of test results processing using non-linear DCB specimen was created.

6. The results confirm the suitability of the nonlinear model of DCB specimen for determination of the G_{Ic} quantity of a composite within the limits of applicability of the standard test methods based on the Euler theory of bending of beams [6].

7. A satisfactory result can be obtained by using an equation that implies correction of the formal expression of G_{Ic} according to the linear model by its multiplication by the standard correction factor [6].

8. To test highly flexible DCB samples, the most reliable estimates of parameter G_{Ic} can be obtained by using the accurate nonlinear model [6].

5. BIBLIOGRAPHY

1. J. M. Hodginson. Mechanical Testing of Advanced Fibre Composites. Cambridge, England. 2000, pp. 170–210.
2. A. Szekrényes. Overview on the Experimental Investigations of the Fracture Toughness in Composite Materials. *Submitted to HEJ*. 2002, pp. 1–9. Manuscript no.: MET-020507-A
3. V. Pavelko. Behavior of Thin-Film-Type Delamination of Layered Composite in Post-Buckling. *Advanced Materials Research.* 2013, vol. 774-776, pp. 1312–1321. Available from: doi: 10.4028/www.scientific.net/AMR.774-776.1312.
4. V. Pavelko, I. Pavelko, M. Smoļaņinovs. Large Deformation and Failure of Thin-Walled Film at the Post-Buckling Delamination. *Key Engineering Materials*. 2014, vol. 577–578, pp. 497–500. Available from: doi: 10.4028/www.scientific.net/KEM.577-578.497
5. Standard Test Method for Mode I Interlaminar Fracture Toughness of Unidirectional FibreReinforced Polymer Matrix Composites, D 5528, *American Society for Testing and Materials International*. ASTM. 1994.
6. Pavelko V., Lapsa K., Pavlovskis P. Determination of the Mode I Interlaminar Fracture Toughness by using a Nonlinear Double-Cantilever Beam Specimen. *Mechanics of Composite Materials*. 2016, vol. 52, no. 3, pp. 347–358. Available from: doi: 10.1007/s11029-016-9587-y
7. Kim Hyoung Seop. On the rule of mixtures for the hardness of particle reinforced composites. *Materials Science and Engineering*. 2000, vol. 289, no. 1–2, pp. 30–33. Available from: doi: 10.1016/S0921-5093(00)00909-6
8. Miller T. C., Liu C. T. Pressure effects and fracture of a rubbery particulate composite. *Experimental Mechanics*. 2001, vol. 41, pp. 254–259. Available from: doi: 10.1007/BF02323142
9. V. Pavelko. Application of the nonlinear model of a beam for investigation of interlaminar fracture toughness of layered composite. *Key Engineering Materials*. 2015, vol. 665, pp. 273–276. Available from: doi: 10.4028/www.scientific.net/KEM.665.273
10. C. Prasanth, S. Ravindranath, A. Samraj, T. Manikandan. Mode-I fracture analysis of thermally aged of glass and glass-carbon hybrid composites. *International Journal of Innovative Technology and Exploring Engineering*. 2014, vol. 3, no. 10, pp. 84–89.
11. Pavelko V., Lapsa K., Pavlovskis P. The Effect of Plasticity to Interlaminar Fracture Toughness of Adhesive Bond of Composite. IOP Conference Series: *Materials Science and Engineering*. 2017, vol. 251: 3rd International Conference on Innovative Materials, Structures and Technologies (IMST 2017), pp. 012081–012081. ISSN 1757-8981. e-ISSN 1757-899X. Available from: doi:10.1088/1757-899X/251/1/012081
12. S. P. Timoshenko, J. M. Gere. Theory of Elastic Stability 2nd Edition. *McGraw-Hill Book Company*, Toronto (1961) Chapter 2.
13. International Organization for Standardization, ISO 15024. Fibre-reinforced plastic composites – Determination of mode I interlaminar fracture toughness, G_{IC}, for unidirectionally reinforced materials. 2001.

Pēteris Pavlovskis was born in 1989 in Riga. He obtained a Professional Bachelor's degree in Aircraft Engineering in 2012 and a Professional Master's degree in Aircraft Engineering in 2014 from Riga Technical University. He has worked as an engineer at the Ultralight Aircraft Manufacturing in Ādaži, as well as a mechanical engineer of designing vertical wind tunnels at Aerodium Technologies Ltd. Since 2020, he has been a technical director of "LGK Atrakcijas" Ltd providing the services of Sigulda Cable Car. Since 2020, he has been also a researcher with Riga Technical University. His research interests are related to composite materials, mechanical engineering, and training of students.